JOURNAL OF SOLID STATE CHEMISTRY **32**, 343–350 (1980)

Thermodynamics of Ordering in β-$Li_xV_2O_5$ Lithium–Vanadium Oxide Bronzes

A. V. POPOV, YU. G. METLIN, AND YU. D. TRETYAKOV

Chemistry Department, Moscow State University, Moscow 117234, USSR

Received August 13, 1979

The thermodynamics of $Li_xV_2O_5$ bronzes have been studied by electrochemical titration in galvanic cells reversible with respect to lithium. The relative partial molar quantities $\Delta\bar{G}_{Li}(x)$, $\Delta\bar{H}_{Li}(x)$, and $\Delta\bar{S}_{Li}(x)$ of litium in β-$Li_xV_2O_5$ bronze have been determined. Some ordering process is proved to take place in the $Li_{0.33}V_2O_5$ bronze. A lithium disordering model is proposed based on available crystallochemical data and presently obtained thermodynamic data. The suggested model is suitable for description of experimental lithium activity values in the wide range of β-$Li_xV_2O_5$ homogeneity. The evaluated disordering constant K_1 amounted to $\log K_1 = -5.14 \pm 0.18$. The model calculation of entropy is consistent with the experimental data.

Introduction

Lithium–vanadium bronze β-$Li_xV_2O_5$ is a nonstoichiometric compound with a wide homogeneity range: $0.22 < x < 0.49$, corresponding to variable lithium content (*1*). Featuring both electronic and lithium ionic conductivity allows this bronze to be used as a solid solution cathode in high-energy secondary batteries (*2*). The lithium ion mobility in the β-$Li_xV_2O_5$ bronze makes it possible to use this compound as a selective lithium electrode in chemical analyses even at ambient temperatures (*3*).

The surprising properties of β-$Li_xV_2O_5$ bronze have attracted great attention from investigators (*4, 5*). The possibility of using this bronze as a cathode in current sources stimulated recent thermodynamic and thermochemical studies of lithium–vanadium bronzes. Several investigations are carried out in this direction including calorimetric solution heat measurements at ambient temperatures (*6, 7*), and coulometric titration of β-$Li_xV_2O_5$ in lithium-reversible galvanic cells at elevated temperatures (*8*).

In the present work we have attempted to study the thermodynamics of β-$Li_xV_2O_5$ bronze at ambient temperatures in detail. This study was carried out by the emf method using coulometric titration in galvanic cells reversible with respect to lithium. We expected that this investigation would give some information about lithium ordering in β-$Li_xV_2O_5$. The structure of this bronze provides the possibility of some ordering but the high-temperature thermodynamic data (*8*) give evidence of the absence of any ordering at elevated temperatures.

Experimental

1. Sample Preparation

To synthesize the $Li_{0.26}V_2O_5$ bronze, a mixture of appropriate amounts of V_2O_5 and Li_2CO_3 was ground carefully under an acetone layer. The dried powder was pressed into pellets (6 mm in diameter, 1 to 2 mm

0022-4596/80/060343-08$02.00/0

thick) at 500 kG/cm^2. The pellets were sintered at 560 to 570°C for 10 hr under a nitrogen flow:

$$0.13\ Li_2CO_3 + V_2O_5 \rightarrow Li_{0.26}V_2O_5 + 0.13\ CO_2(g) + 0.065\ O_2(g). \quad (1)$$

The phase composition of the samples was examined by X-ray powder diffraction with a URS-50 IM diffractometer, using Fe*Kα* radiation.

Porosity of the samples amounted to 30%.

2. *Apparatus and Procedure*

The thermodynamic study was carried out by emf measurements in Li-reversible galvanic cells:

$$Pt,\ Li_{(s)}|Li^+|Li_{0.26}V_2O_{5(s)},\ Pt \qquad (A)$$

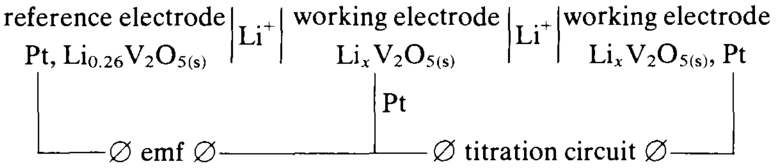

(B)

The 0.5 M solution of $LiClO_4$ in dimethyl sulfoxide $(CH_3)_2SO$(DMSO) was used as a liquid electrolyte. According to the published data (*9*), the solutions of $LiClO_4$ in DMSO exhibit sufficiently high ionic conductivity. Being submerged in $LiClO_4$–DMSO solution, pure metallic lithium is rather stable due to formation of a protecting film layer (*10*).

Cell (A) was used for determination of the thermodynamic properties of the β-$Li_{0.26}V_2O_5$ bronze which was employed further as the reference electrode in cell (B). The working electrode composition of cell (B) was changed by coulometric titration. The definite amount of charge, being passed through the titration circuit, varied the composition of both working electrodes due to electrochemical transfer of lithium ions across the electrolyte. High lithium ion mobility in $Li_xV_2O_5$ (*11*) provided sufficiently fast uniform Li^+ ion distribution throughout the working electrodes. Coulometric titration was performed by discrete steps in both directions, emf value being determined at every step at temperatures of 25 and 50°C. To reach equilibrium cell (B) after coulometric tritration required 15–20 hr at constant temperature. On the contrary, upon altering the temperature, emf equilibrium appeared to follow temperature equilibrium very rapidly (2 to 5 min).

In principle, the present study could be performed using cell (A) only. However, our preliminary experiments showed that equilibrium emfs of cell (A) remained constant for 50–60 hr only. Reaction is likely to take place between lithium and DMSO resulting in progressive growth of the product layer, leading to deviation of the emf from the equilibrium value. But the investigation of the whole β-$Li_xV_2O_5$ homogeneity range requires 3–4 weeks. The solution of $LiClO_4$ in DMSO being stable concerning β-$Li_xV_2O_5$ bronze over a long period of time, cell (B) was created for coulometric titration.

The cell emfs were measured by compensation using a R37-1 potentiometer with a F116/2 DC amplifier as a null indicator. Sensibility of emf measurements amounted to 0.005 mV. Criterion of equilibrium was emf constancy within ±0.1 mV for 2 hr at a constant temperature, and emf reproducibility both at stepped titration in the two directions and at repeated heating and cooling of the cell. The titration current was maintained constant (200 ± 1) μA by a P-

5827M potentiostat. The temperature of the cells was kept constant (±0.05°C) by a TS-15 thermostat. The samples (50–100 mg) were weighed if necessary on a VLR-200 analytical balance to an accuracy of ±0.1 mg.

Results

Equilibrium emf values of cells (A) and (B) at temperatures of 25 and 50°C are given in Table I. The emf values of an imaginary cell,

$$\mathrm{Pt,\ Li_{(s)}|Li^+|Li_xV_2O_{5(s)},\ Pt,} \qquad \text{(C)}$$

necessary for evaluating thermodynamic functions were calculated by summarizing emfs of cell (B) at different x with emf of cell (A) for corresponding temperatures. The calculated emfs of cell (C) (they are omitted) allowed us to evaluate the relative partial molar quantities $\Delta\bar{G}_{\mathrm{Li}}(x)$, $\Delta\bar{S}_{\mathrm{Li}}(x)$, and $\Delta\bar{H}_{\mathrm{Li}}(x)$ in the range $0.02 \leqslant x \leqslant 0.64$ according to the well-known formulas:

$$\Delta\bar{G}_{\mathrm{Li}}(x) = -FE(x), \qquad (2)$$

$$\Delta\bar{S}_{\mathrm{Li}}(x) = F\left(\frac{\partial E(x)}{\partial T}\right)_x, \qquad (3)$$

$$\Delta\bar{H}_{\mathrm{Li}}(x) = \Delta\bar{G}_{\mathrm{Li}}(x) + T\Delta\bar{S}_{\mathrm{Li}}(x), \qquad (4)$$

where

$\Delta\bar{G}_{\mathrm{Li}}(x)$ is the relative partial molar free energy of lithium,

$\Delta\bar{S}_{\mathrm{Li}}(x)$ is the relative partial molar entropy of Li,

$\Delta\bar{H}_{\mathrm{Li}}(x)$ is the relative partial molar enthalpy of Li,

$E(x)$ is emf of cell (C),

$F = 96{,}495$ C/mole is Faraday's constant.

The results are plotted in Fig. 1.

Lithium activities in the β-$Li_xV_2O_5$ bronze are listed in Table II calculated as follows:

$$a_{\mathrm{Li}}(x) = \exp\left(-\frac{\Delta\bar{G}_{\mathrm{Li}}(x)}{RT}\right), \qquad (5)$$

where $R = 8.3148$ *J/mole · K*.

TABLE I

EMFs of Cells (A) and (B) at 25 and 50°C

	emf (mV)				
x	$t = 25$°C	$t = 50$°C	x	$t = 25$°C	$t = 50$°C
—	3630.2	3626.5	0.31	−53.0	−55.1[a]
0.02	182.3	195.8	0.32	−78.9	−77.5
0.04	138.1	150.7	0.325	−120.1	−115.8
0.05	126.3	138.0	0.33	−165.0	−157.8
0.07	111.7	122.9	0.34	−193.6	−182.9
0.08	106.1	117.0	0.35	−205.1	−194.3
0.11	87.4	96.5	0.36	−215.3	−204.8
0.16	58.6	66.1	0.38	−217.5	−211.6
0.17	43.0	50.1	0.40	−219.3	−213.1
0.19	33.0	38.4	0.41	−216.8	−210.7
0.20	32.1	37.1	0.43	−218.1	−211.9
0.21	24.4	29.0	0.45	−223.0	−221.6
0.25	6.9	7.6	0.49	−257.2	−256.2
0.27	−8.0	−8.5	0.55	−305.8	−305.5
0.29	−24.8	−26.4	0.59	−343.7	−344.3
0.30	−32.0	−34.1	0.64	−404.1	−406.4

[a] EMF of cell (A).

An entropy change corresponding to the reaction

$$x\mathrm{Li_{(s)}} + \mathrm{V_2O_{5(s)}} \rightarrow \mathrm{Li}_x\mathrm{V_2O_{5(s)}} \qquad (6)$$

was calculated according to equation

$$\Delta S = \int_0^x \Delta\bar{S}_{\mathrm{Li}}(x)\,dx. \qquad (7)$$

The results are plotted in Fig. 2.

Discussion

1. Phase Relations in the $Li_xV_2O_5$ Bronze upon Coulometric Titration

First of all, considering the obtained data makes it possible to characterize the processes occurring in the bronze upon coulometric titration.

According to the V_2O_5–LiV_2O_5 (Fig. 3) phase diagram, two horizontal plateaus are expected on the curves of partial molar quantities $\Delta\bar{G}_{\mathrm{Li}}(x)$, $\Delta\bar{H}_{\mathrm{Li}}(x)$, $\Delta\bar{S}_{\mathrm{Li}}(x)$,

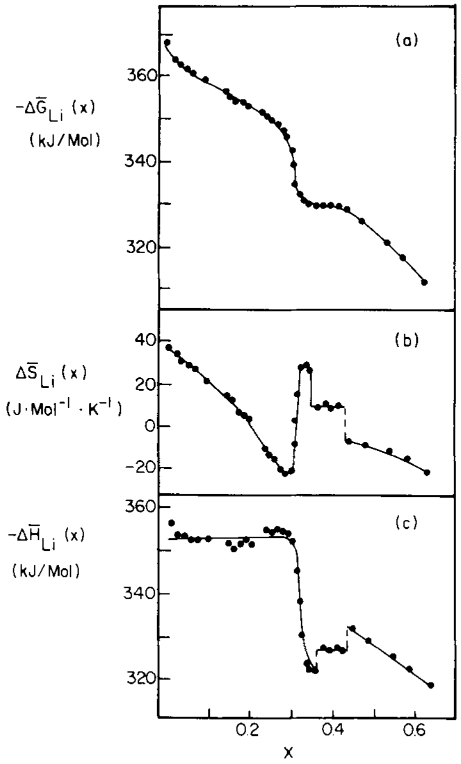

FIG. 1. Relative partial molar quantities of lithium in the β-$Li_xV_2O_5$ bronze VS x at 25°C.

TABLE II

LITHIUM ACTIVITY a_{Li} AND LOGARITHM OF DISORDERING CONSTANT $\log K_I$ FOR β-$Li_xV_2O_5$ ($0.02 \leq x \leq 0.36$) AT 25°C

x	a_{Li}	$-\log K_I$
0.02	3.68×10^{-65}	5.44
0.04	2.05×10^{-64}	5.20
0.05	3.20×10^{-64}	5.20
0.07	5.73×10^{-64}	5.40
0.08	7.13×10^{-64}	5.44
0.11	1.47×10^{-63}	5.49
0.16	4.53×10^{-63}	5.40
0.17	8.31×10^{-63}	5.02
0.19	1.23×10^{-62}	5.02
0.20	1.27×10^{-62}	5.13
0.21	1.71×10^{-62}	5.02
0.25	3.38×10^{-62}	5.11
0.26	4.43×10^{-62}	5.08
0.27	6.05×10^{-62}	5.02
0.29	1.16×10^{-61}	4.96
0.30	1.54×10^{-61}	5.08
0.31	3.48×10^{-61}	4.86
0.32	9.55×10^{-61}	4.99
0.325	4.74×10^{-60}	—
0.33	2.76×10^{-59}	5.11
0.34	8.25×10^{-59}	5.08
0.35	1.29×10^{-58}	4.96
0.36	1.93×10^{-58}	4.96

corresponding to two-phase equilibrium mixtures $\alpha+\beta$ ($0.04<x<0.22$) and $\beta+\gamma$ ($0.49<x<0.88$). But these plateaus were not indicated on experimental plots in the above-mentioned ranges. The X-ray phase analysis of electrochemically prepared $Li_{0.02}V_2O_5$ and $Li_{0.64}V_2O_5$ bronzes detected the β-phase only, without traces of the α- and γ-phases. It is known also (*12*) that the electrochemical titration of α-$Li_xV_2O_5$ down to $x=1$ at ambient temperatures does not lead to the appearance of β- and γ-phases. The listed data allow us to conclude that the phase trtansitions $\beta \rightleftarrows \alpha$ and $\beta \rightleftarrows \gamma$ are kinetically hindered at ambient temperature. Consequently, the results of the present work cannot be compared directly with the phase diagram in Fig. 3, which reflects only high-temperature equilibrium of the V_2O_5–LiV_2O_5 system.

At the same time, equilibrium connected with lithium exchange between the electrolyte and the bronze is reached comparatively rapidly as is evidenced by reversibility of galvanic cells (A) and (B). Thus, the

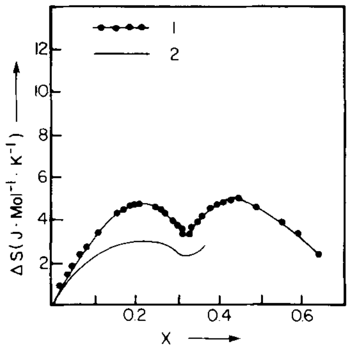

FIG. 2. The entropy change of the reaction (6) VS x: 1, evaluated from the experimental data; 2, calculated according to Eq. (23).

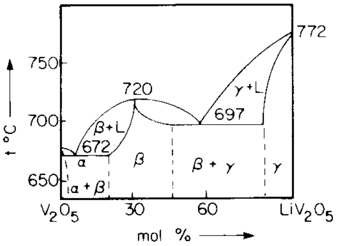

FIG. 3. Phase diagram of the V_2O_5–LiV_2O_5 system (1).

studied system is in partial equilibrium relative to lithium whereas equilibrium associated with a rearrangement of the vanadium–oxygen covalent framework is frozen. Partial equilibria are known to be studied by thermodynamic methods in the same way as complete equilibria. This allows us to consider the data obtained as quasi-equilibrium data, although the β-$Li_xV_2O_5$ bronze is probably metastable relative to α- and γ-phases at $x < 0.22$ and $x > 0.49$, respectively.

As fas as we know, $Li_xV_2O_5$ bronzes with β-phase structure and lithium content (x) greater than 0.5 and less than 0.2 seem to have been prepared for the first time.

As is known from published data (13), at low temperatures β-$Li_xV_2O_5$ bronze is not completely homogeneous. Pure β-phase exists at $x < 0.37$ only. At $x > 0.44$, a β'-phase occurs, featuring the other distribution of Li^+ ions within the same V_2O_5 framework. Therefore, a horizontal plateau on the experimental curve $\Delta\bar{G}_{Li}(x)$ in the range $0.36 < x < 0.44$ (Fig. 1a) is consistent with an equilibrium mixture of β- and β'-phases.

2. *Ordering in the Structure of β-$Li_xV_2O_5$*

There are certain anomalies on the experimental plots of $\Delta\bar{G}_{Li}(x)$ and $\Delta\bar{S}_{Li}(x)$ near $x = 0.33$. Indeed, $\Delta\bar{G}_{Li}(x)$ (Fig. 1a) exhibits a curve bend, and $\Delta\bar{S}_{Li}(x)$ (Fig. 1b) gives a curve drop close to discontinuity of the function. This behavior of thermodynamic functions presents some evidence that ordering indeed takes place in the $Li_{0.33}V_2O_5$ bronze.

Using thermodynamic data presently obtained along with crystallochemical data (14) we attempted to evaluate the mechanism and extent of lithium ordering in the structure of β-$Li_xV_2O_5$. A disordering model based on the statistic thermodynamics approach within quasi-chemical approximation was constructed.

The β-$Li_xV_2O_5$ bronze crystallizes in the monoclinic system with space group A^2/m (structure group $Na_{0.33}V_2O_5$), and the unit cell contains six formula units of $Li_xV_2O_5$. Lithium atoms are ionized completely and exist as Li^+ in this structure, the corresponding number of electrons being localized on vanadium atoms, decreasing their oxidation number from 5+ to 4+ (4). Thus $Li_xV_2O_5$ contains a variable quantity of V^{4+} equivalent to lithium content. As represented in Fig. 4, the vanadium atoms are in quite distorted octahedra which form strings along the y-axis, leaving tunnels along the y-axis in which the lithium ions lie. There are four possible sites for lithium per unit cell. These sites occur in pairs about 3 Å apart, and the distance between pairs amounts to 3.6 Å (Fig. 5).

For the $Li_{0.33}V_2O_5$ bronze, the number of lithium ions is half the number of possible sites. In this case, three alternatives for the lithium ion arrangement exist (Fig. 6): zigzag (a), one over another (b), or random (c). No direct experimental evidence has been available until now concerning the manner of arrangement. It is known only that the lithium ion arrangement in the whole

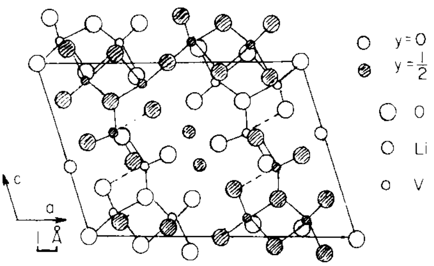

FIG. 4. Projection of the β-$Li_xV_2O_5$ structure onto the plane (010) (14).

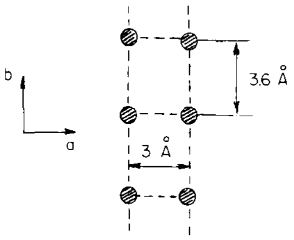

FIG. 5. Lithium ion positions in the channel of β-$\mathrm{Li_{2/3}V_2O_5}$ projected on the plane (001).

β-$\mathrm{Li_{0.33}V_2O_5}$ structure is disordered as evidenced by absence of superstructure reflections even on overexposed X-ray patterns (*15*). However, a disordered arrangement (Fig. 6c) cannot be assumed as proven. If lithium ions order within a single channel, disordering through the whole crystal may be attained by a random orientation of chains in neighboring tunnels relative to one another. Such a disorder retains the space group A^2/m for the whole crystal, but the unit cell space group falls to *Am* (*15*).

The thermodynamic consideration of ordering in β-$\mathrm{Li_xV_2O_5}$ attempted presently requires one to choose the common system for describing possible structures using the terms "point defect" and "associate." The zigzag arrangement (Fig. 6a) is selected as a basic structure consistent with the minimum of Coulomb repulsion energy. The absence of correlation between lithium ion arrangements in adjacent channels is postulated. Each site pair in the zigzag structure (Fig. 6a) is considered as an associate $(\mathrm{Li_{Li}}, V_i)^x$ where V_i is the vacant site adjacent to the occupied site, $\mathrm{Li_{Li}}$. With this approach, the transition to the disordered structure (Fig. 6c) is a Frenkel disordering:

$$(\mathrm{Li_{Li}}, V_i)^x \rightarrow (\mathrm{Li}_i, V_{\mathrm{Li}})^x, \qquad (8)$$

whereas the structure in Fig. 6b is a superstructure with strict alternation of $(\mathrm{Li_{Li}}, V_i)^x$ and $(\mathrm{Li}_i, V_{\mathrm{Li}})^x$.

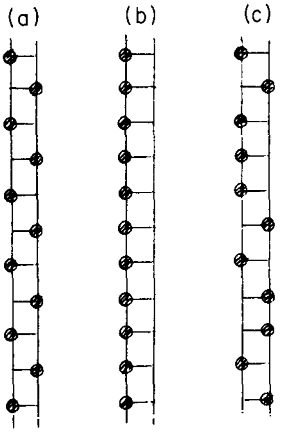

FIG. 6. Possible lithium ion distributions in the channels of β-$\mathrm{Li_{1/2}V_2O_5}$ bronze (*11*).

Another type of disordering considered presently is translation of the lithium ion from one unit cell to another along the channel (Fig. 7):

$$2(\mathrm{Li_{Li}}, V_i)^x \rightarrow (\mathrm{Li_{Li}}, \mathrm{Li}_i)^{\cdot} + (V_{\mathrm{Li}}, V_i)'. \qquad (9)$$

The processes illustrated by Eqs. (8) and (9) are denoted as disorderings I and II, respectively.

It should be noted that, if disordering I or II takes place even to a small extent, the long-range order is disturbed in the channel and the difference is lost between $\mathrm{Li_{Li}}$ and Li_i as well as between V_i and V_{Li} (see Fig. 6c and Fig. 7). Therefore, we drop indexes Li and *i* while representing the process of disordering II:

$$2(\mathrm{Li}, V)^x \rightarrow (\mathrm{Li}, \mathrm{Li})^{\cdot} + (V, V'). \qquad (10)$$

Equation (10) is written taking into account possible disordering I but independent of the extent of this disordering.

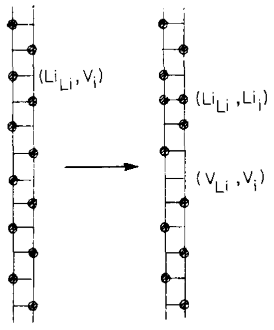

FIG. 7. The mechanism of disordering II.

NMR data on Li^7 in $Li_{0.35}V_2O_5$ are consistent with both disordering processes proposed presently, though the authors (*16*) did not discuss them in terms of "ordering–disordering".

The transition from $Li_{0.33}V_2O_5$ to bronzes of another composition is descrbed as follows:

$$\mathrm{Li}_{(s)} + (\mathrm{Li}, V)^x \rightarrow (\mathrm{Li}, \mathrm{Li})^{\cdot} + e' \qquad (11)$$

$$(\mathrm{Li}, V)^x + e' \rightarrow (V, V)' + \mathrm{Li}_{(s)}. \qquad (12)$$

Equation (11) corresponds to intercalation of lithium in the bronze, and Eq. (12) to removing of lithium.

The quasi-chemical approximation (*17, 18*) being used here allows us to express the equilibrium constants of reactions (10), (11), and (12) as:

$$K_1 = C_0 C_2 C_1^{-2}, \qquad (13)$$

$$K_2 = C_2 n a_{\mathrm{Li}}^{-1} C_1^{-1}, \qquad (14)$$

$$K_3 = a_{\mathrm{Li}} n^{-1} C_0 C_1^{-1}, \qquad (15)$$

where

K_1, K_2, and K_3 are equilibrium constants,

a_{Li} is lithium activity,

n is electron concentration, mole/mole of bronze,

$$\left.\begin{array}{l} C_0 = [(V, V)'] \\ C_1 = [(\mathrm{Li}, V)^x] \\ C_2 = [(\mathrm{Li}, \mathrm{Li})^{\cdot}] \end{array}\right\} \text{ in moles per 1 mole of bronze}$$

The material balance equations are:

$$C_0 + C_1 + C_2 = x_0, \qquad (16)$$

$$C_1 + C_2 = x, \qquad (17)$$

where x_0 is the stoichiometric concentration, i.e., the lithium content that permits the full ordering ($x_0 = 0.33$).

Solution of the system of Eq. (13–17) allows us to find concentrations of the structure species and the ratio $a_{\mathrm{Li}}/a_{\mathrm{Li}}^*$ as a function of composition parameter x (a_{Li}^* is the lithium activity at stoichiometric concentration). The task is simplified by introducing suitable approximations if the self-disordering constant K_1 is fairly small. So, x being close to x_0, the assumption $[(\mathrm{Li}, V)] \approx x_0$ leads to the following equations:

$$C_0 = (x_0 - x)/2 + ((x_0 - x)^2/4 + K_1 x_0^2)^{1/2}, \qquad (18)$$

$$C_2 = (x - x_0)/2 + ((x - x_0)^2/4 + K_1 x_0^2)^{1/2}, \qquad (19)$$

$$a_{\mathrm{Li}}/a_{\mathrm{Li}}^* = (x - x_0) x_0^{-1} K_1^{-1/2}/2 + ((x - x_0)^2 K_1^{-1} x_0^{-2}/4 + 1)^{1/2}. \qquad (20)$$

If the x value greatly differs from x_0 the suggestion that $[(\mathrm{Li}, V)] \approx x_0$ is quite wrong. In such case in Eqs. (16) and (17) one can set these $[(\mathrm{Li}, \mathrm{Li})^{\cdot}] = 0$ on $x < x_0$ or, in contrast, $[(V, V)'] = 0$ upon $x > x_0$. Under these assumptions, one obtains:

$$a_{\mathrm{Li}}/a_{\mathrm{Li}}^* = x^2 K_1^{1/2} x_0^{-1} (x_0 - x)^{-1} \quad \text{if } x < x_0, \qquad (21)$$

$$a_{\mathrm{Li}}/a_{\mathrm{Li}}^* = x(x - x_0) K_1^{-1/2} x_0^{-1} (2x_0 - x)^{-1} \quad \text{if } x > x_0. \qquad (22)$$

Equations (18–22) were used to evaluate corresponding values of the disordering constant K_1 from exprimental lithium activities. The value $x_0 = 0.325$ corresponding to the curve bend of the $\Delta\bar{G}_{\mathrm{Li}}(x)$ function (Fig. 1a) was chosen as the stoichiometric concentration. This value of x_0 is in good agreement with the theoretical value $x_0 = \frac{1}{3} = 0.33(3)$.

The evaluated values of $\log K_1$ given in Table II keep roughly constant magnitude $\log K_1 = -5.14 \pm 0.18$ near as well as far from the stoichiometric concentration. Therefore, the proposed disordering model is useful for describing the experimental data within the wide range of lithium content corresponding to the pure β-phase without β'-phase. To prove the consistency of this model, a back-calculation of $\Delta\bar{G}_{\mathrm{Li}}(x)$ was made according to Eqs. (18–22) and (5) using the experimental values $a_{\mathrm{Li}}^* = 4.74 \times 10^{-60}$,

$\log K_1 = -5.14$ (solid curve in the range 0.02 to 0.36 in Fig. 1a). The back-calculated curve is seen to follow the experimental points, exhibiting no systematic deviations.

The β-$Li_xV_2O_5$ disordering model described above makes it possible to evaluate the configuration entropy change in reaction (6) from the Bolzmann formula:

$$\Delta S = R \ln W$$
$$= kN_A \ln N!2^{N_1}N_0!^{-1}N_1!^{-1}N_2!^{-1}, \qquad (23)$$

where

N_0, N_1, N_2 = number of (V, V), (Li, V), and (Li, Li) "associates" per mole of bronze,

$N_i = N_A \cdot C_i$ $(i = 0, 1, 2)$,

$N = N_A \cdot x_0$,

$N = N_0 + N_1 + N_2$,

N_A = Avogadro constant,

k = Bolzmann constant.

The results are plotted in Fig. 2. The calculated curve is seen to reproduce the shape of the experimental curve, especially near $x = 0.33$. The marked difference $\Delta S_{exp} - \Delta S_{calc}$ is evidence that the electronic and vibration entropies make a noticeable contribution to the whole entropy of the bronze.

Conclusions

The thermodynamic data presently obtained prove that some ordering process takes place in the $Li_{0.33}V_2O_5$ bronze. A lithium ion disordering model of β-$Li_xV_2O_5$ is built up using these thermodynamic data along with crystallochemical data (*14*). The proposed model is consistent with experimental lithium activity magnitudes. The evaluated disordering constant K_1 remains roughly constant ($\log K_1 = -5.14 \pm 0.18$) over the wide homogeneity range of β-$Li_xV_20_5$. The calculation of entropy based on this model correlates with the experimenta data.

Acknowledgments

The authors with to thank Professor V. A. Geideric and Drs. J. A. Kessler and A. R. Kaul for many helpf discussions.

References

1. A. A. Fotiev, *Zh. Fiz. Khim.* **47**, 1558 (1973).
2. U. S. Patent No. 3,970,473, July 20, 1976.
3. A. G. Koksharov, *Uch. Zap. Perm. Univ. Khi* **178**, 117 (1968).
4. P. Hagenmüller, *in* "The Chemistry of Extended Defects in Non-Metallic Solids" (L. R. Eyrin and M. O'Keefe, (Eds.)), North-Holland, Amsterdam (1970).
5. D. J. Bevan and P. Hagenmüller, *in* "Non Stoichiometric Compounds: Tungsten Bronze Vanadium Bronzes and Related Compounds," Vo 1, Pergamon Texts in Inorganic Chemistr Pergamon, Oxford (1973).
6. E. D. Pletneva, M. Ya. Khodos, A. A Fotiev, and V. L. Volkov, *Izv. Akad. Nauk SSSR Ser. Khim.* **7**, 1669 (1977).
7. S. E. Filippova, J. A. Kessler, Yu. D Tretyakov, and I. V. Gordeyev, *Neor Mater.* **2**, 320 (1979).
8. A. V. Popov, Yu. G. Metlin, and Yu. D Tretyakov, *J. Solid State Chem.* **31**, 23 (1980).
9. H. Lund and P. Iversen, *in* "Organic Electrochemistry" (M. M. Baizer, Ed.), Dekker, Ne York (1973).
10. J. O. Besenhard and G. Eichinger, *J. Electroanal. Chem.* **68**, 1 (1976).
11. M. S. Whittingham and R. A. Huggins, *i* "Fast Ion Transport in Solids" (W. Van Gool, Ed. Proceedings, NATO Sponsored Advanced Stud Institute on Fast Ion Transport in Solids, Solid Stat Batteries and Devices, Elsevier, Amsterda (1973).
12. M. S. Whittingham, *J. Electrochem. Soc.* **12** 315 (1976).
13. J. Galy, J. Darriet, and P. Hagenmülle *Rev. Chim. Miner.* **8**, 509 (1971).
14. A. Gardy, J. Galy, A. Casalot, and Pouchard, *Bull. Soc. Chim. Fr.* **4**, 1056 (1965
15. R. P. Ozerov, *Kristallokhimiya* **2**, 226 (1957).
16. J. Gendell, R. M. Cotts, and M. J. Sienko, *Chem. Phys.* **37**, 220 (1962).
17. C. Wagner and W. Schottky, *Z. Phys. Che B* **11**, 163 (1931).
18. W. Schottky, *Z. Phys. Chem. B* **29**, 335 (1935